

7. DATA REPORT: CHEMICAL AND ISOTOPIC (S, Sr) COMPOSITION OF ANHYDRITE FROM ODP LEG 193, PACMANUS HYDROTHERMAL SYSTEM, MANUS BASIN, PAPUA NEW GUINEA¹

Wolfgang Bach,² Stephen Roberts,³ and Ray A. Binns⁴

ABSTRACT

Sr and S isotope data as well as trace element data for anhydrite samples from Sites 1188 and 1189 in the PACMANUS hydrothermal area are presented here. $^{87}\text{Sr}/^{86}\text{Sr}$ ratios range from 0.7050 to 0.7086, suggesting that the anhydrites precipitated from fluids that were variably influenced by entrained seawater (0%–89%). $\delta^{34}\text{S}$ values range between 18.1‰ and 22.5‰, indicating the main source of sulfate is seawater that may be affected to small extents by sulfide oxidation or magmatic sulfate input ($\delta^{34}\text{S} < 21\text{‰}$) and minor sulfate reduction ($\delta^{34}\text{S} > 21\text{‰}$). Rare earth element (REE) concentrations are highly variable, particularly at Site 1188. Chondrite-normalized REE pattern shapes comprise light REE enriched, light REE depleted, mid-REE enriched, and variable positive and negative Eu anomalies. Significant correlations between trace element and isotopic compositions are lacking. Anhydrite from Site 1188, a site of diffuse venting, has systematically lower $\delta^{34}\text{S}$ and higher Sr contents and somewhat lower average $^{87}\text{Sr}/^{86}\text{Sr}$ than anhydrite from Site 1189. This is possibly a consequence of the different fluid flow regime with diffuse flow at Site 1188 and focused flow at Site 1189.

¹Bach, W., Roberts, S., and Binns, R.A., 2005. Data report: Chemical and isotopic (S, Sr) composition of anhydrite from ODP Leg 193, PACMANUS Hydrothermal System, Manus Basin, Papua New Guinea. *In* Barriga, F.J.A.S., Binns, R.A., Miller, D.J., and Herzig, P.M. (Eds.), *Proc. ODP, Sci. Results*, 193, 1–23 [Online]. Available from World Wide Web: <http://www-odp.tamu.edu/publications/193_SR/VOLUME/CHAPTERS/214.PDF>. [Cited YYYY-MM-DD]

²Department of Marine Chemistry and Geochemistry, Woods Hole Oceanographic Institution, Woods Hole MA 02543, USA.

wbach@whoi.edu

³Southampton Oceanography Centre, Empress Dock, University of Southampton SO14 3ZH, United Kingdom.

⁴CSIRO Exploration and Mining, PO Box 136, North Ryde NSW 2113, Australia.

Initial receipt: 12 March 2004

Acceptance: 13 October 2004

Web publication: 26 January 2005

Ms 193SR-214

INTRODUCTION

The PACMANUS hydrothermal system in the eastern Manus Basin is hosted by felsic volcanic rocks and thus provides the opportunity to examine contrasts with basalt-hosted systems at mid-ocean ridges. The accretion of new crust in the eastern Manus Basin differs markedly from mid-ocean-ridge settings, and examination of the consequences for hydrothermal alteration patterns may broaden our understanding of links between magmatism, tectonism, and hydrothermalisms in modern and ancient hydrothermal systems. The vesicular and brecciated nature of lava flows at PACMANUS (Paulick et al., 2004) have consequences for the patterns of fluid flow, the pervasiveness of hydrothermal alteration, and the efficiency of metal leaching by hydrothermal fluid systems. Moreover, the situation of the PACMANUS hydrothermal system behind an active island arc and its felsic volcanic affiliation may make it a close analog for many ancient volcanogenic massive sulfide (VMS) ore environments. Chemical and isotopic compositions of anhydrite (and other hydrothermal precipitates) provide valuable tracers for the nature of hydrothermal fluids (e.g., Mills and Elderfield, 1995; Mills and Tivey, 1999; Teagle et al., 1998b; Coggon et al., 2004). Here we present Sr and S isotope data as well as minor and trace element concentrations of anhydrite separated from Ocean Drilling Program (ODP) Leg 193 drill core samples from basement beneath the PACMANUS hydrothermal field in the eastern Manus Basin.

METHODS

Anhydrite samples were separated and analyzed in three different laboratories. At the Woods Hole Oceanographic Institution (WHOI), Massachusetts (USA), Sr isotope and trace element (Sr, Li, Rb, Cs, Ba, La, Ce, Pr, Nd, Sm, Eu, Gd, Tb, Dy, Ho, Er, Yb, Lu, Y, Pb, U, P, and As) analyses were performed. At Southampton Oceanography Center (SOC; UK), Sr and S isotope as well as trace element analyses (Mg, Sr, Rb, Cs, Ba, La, Ce, Pr, Nd, Sm, Eu, Gd, Tb, Dy, Ho, Er, Tm, Yb, Lu, Y, Pb, and U) analyses were carried out. Additional Sr and S isotope analyses were conducted at the Commonwealth Scientific and Industrial Research Organization (CSIRO), New South Wales (Australia).

WHOI

Preparation

Anhydrite crystals were carefully hand-picked under a binocular microscope. Several milligrams of anhydrite were gently crushed in a Savillex Teflon beaker and dissolved in dilute HCl at 60°C overnight.

Trace Element Analyses

Following sample dissolution, most of the HCl was removed by two cycles of heating to incipient dryness and addition of 1-N HNO₃. Sample solutions were centrifuged and injected (via a nebulizer) into a Finnigan element inductively coupled plasma–mass spectrometer (ICP-MS) at WHOI that was calibrated by running matrix-matched trace element standard solutions. Tm and In spikes were added as internal standards. Isobaric mass interferences were checked (e.g., BaO and BaOH

interferences on Eu), but oxide production was found negligible, due to the use of a nebulizer. Blanks were monitored and a blank correction was applied. Reproducibility of the data is better than 3%–8%.

Sr Isotope Analyses

About 10 mg of hand-picked anhydrite crystals were dissolved with 2.5-N HCl in Savillex Teflon beakers. A Sr spike was added prior to dissolution to determine Sr concentrations by isotope dilution. Strontium was separated on quartz columns with a 5-mL resin bed of AG50W-X8 200–400 mesh. Sr isotopes were analyzed at WHOI with a VG 354 thermal ionization mass spectrometer (TIMS). $^{87}\text{Sr}/^{86}\text{Sr}$ ratios are reported relative to National Bureau of Standards (NBS) reference material 987 = 0.71024. External precision (2σ) of Sr isotope analyses is 30 ppm.

SOC

Preparation

Approximately 10–15 mg of anhydrite was weighed into clean Savillex Teflon vials. A 6-mL aliquot of ~2% subboiled nitric acid was added and the samples left to dissolve on a hot plate at 60°C for 10 days.

Trace Elements

Following dissolution, the samples were subsampled for Sr and Mg analysis on a Perkin-Elmer Optima 4300 ICP–atomic emission spectrometer (AES) calibrated using synthetic matrix-matched standards. Rare earth elements (REE) and other trace elements were analyzed on a separate subsample using ICP-MS. Calibration was carried out using a suite of matrix-matched synthetic chondritic pattern standards for REE and international rock standards for trace elements.

Sr Isotopes

Subsamples for strontium isotopes were taken to give ~1 μg of Sr; the Sr was separated using 80l Sr-Spec columns eluted with 3-N nitric acid. The samples were loaded with a Ta activator solution onto single Ta filaments and analyzed on a VG Sector 54 TIMS. The value for NBS-987 during this work was 0.710252 ± 18 on 29 runs.

Sulfur Isotopes

Anhydrite was prepared by microdrilling. Approximately 5–10 mg was required for isotopic analysis. Minor contamination by non S-bearing phases was tolerated and has no effect on the final data. Anhydrite analyses were performed at Scottish Universities Research and Reactor Centre (SURRC; UK) by the technique of Coleman and Moore (1978), in which SO_2 gas is liberated by combustion with excess Cu_2O and silica at 1125°C. Liberated gases were analyzed on a VG Isotech SIRA II mass spectrometer, and standard corrections applied to raw $\delta^{66}\text{SO}_2$ values to produce true $\delta^{34}\text{S}$. The standards employed were the international standards NBS-123 and IAEA-S-3 and the SURRC standard CP-1. These gave $\delta^{34}\text{S}$ values of +17.1‰, –31‰, and –4.6‰, respectively, with 1σ reproducibility better than $\pm 0.2\%$. Data are reported in $\delta^{34}\text{S}$ notation as permil (‰) variations from the Vienna Canyon Diablo troilite (V-CDT) standard.

CSIRO

Preparation

Anhydrite concentrates from selected portions of core were prepared by hand picking under a binocular microscope. After the initial pick, the concentrate was gently ground under acetone and dust removed by elutriation, following which any remaining contaminants (mostly pyrite inclusions) were again hand-picked under the binocular microscope. Where necessary, this was repeated a third time. In this way, concentrates exceeding 99.5% purity and often exceeding 99.9% were obtained. For a few samples with limited quantity, a separate subsample with 1%–2% pyrite contaminant was tolerated for Sr isotope measurements. Bluish gypsum as well as anhydrite was separately picked from Sample 193-1189B-1R-1 (Piece 1A, 0–6 cm); remaining gypsum was removed from the anhydrite concentrate by leaching in boiling water. The concentrate from Sample 193-1189B-3R-1 (Piece 1, 0–11 cm) consisted of 90% gypsum and 10% anhydrite and was submitted in bulk for isotope analysis. The anhydrite concentrate of the thin vein from Sample 193-1188A-17R-1 (Piece 24, 137–140 cm) contained ~10% gypsum and was also submitted in bulk.

For sample dissolution, ~0.01–0.09 g of anhydrite separate was weighed and placed in HCl. The supernatant fluid was decanted ready for cation exchange chromatography. Approximately 0.1g of gypsum was weighed and placed in Milli-Q water to obtain a leachate. The supernatant fluid was decanted, evaporated, and then converted to a chloride form and brought up to final volume in HCl for cation exchange chromatography.

Sr Isotopes

Sr was separated on AG50W-X8 cation exchange resin. The separated Sr was loaded onto a single Ta filament with water and H₃PO₄ and oxidized in air. The isotopic compositions were measured on a VG 354 TIMS fitted with seven collectors. Samples were run in “dynamic” mode with an ion beam intensity of 3×10^{-11} A of ⁸⁸Sr. Six blocks of nine ⁸⁷Sr/⁸⁶Sr ratios were measured, yielding a total of 54 determinations. ⁸⁷Sr/⁸⁶Sr ratios were normalized to ⁸⁶Sr/⁸⁸Sr = 0.1194 using an exponential correction law. Rubidium was monitored continuously throughout the run, and a negligible correction was applied. The raw data were filtered using a 2σ rejection criterion. Measured blanks have a negligible effect on the measured ratios.

The precision of individual analyses at 95% confidence limits, determined as two standard errors of the mean, is typically between 0.0010% and 0.0020% (internal precision). Measurements of the standard reference material NBS-987 were made with each batch of samples, yielding an average ⁸⁷Sr/⁸⁶Sr ratio of 0.710269 ± 18 (1σ; *n* = 33).

Sulfur Isotopes

Sulfate was extracted from the anhydrite concentrates by leaching with distilled and degassed water. One gypsum concentrate was treated briefly to avoid dissolution of anhydrite contaminant. The sulfate solutions were separated from undissolved anhydrite, acidified, and BaSO₄ was precipitated. The dried BaSO₄ precipitate was loaded into a 5-cm-long, 6-mm-diameter quartz tube and dropped into a 9-mm-diameter

quartz tube, the system was evacuated, and the sample was heated to $>1500^{\circ}\text{C}$ using a hydrogen/oxygen torch (Bailey and Smith, 1972). The gaseous products were passed over a hot copper plug (600°C) and separated cryogenically. The volume of SO_2 was measured and transferred to a suitable vessel for mass spectrometry. Prepared gases were analyzed on a Finnigan 252 mass spectrometer in dual inlet mode. Results are reported using the delta notation relative to V-CDT. Replicate analysis of sulfide and sulfate standard materials were better than $\pm 0.2\text{‰}$.

RESULTS

PACMANUS comprises several discrete vent site fields (all on the order of 100–200 m in diameter) over a 3-km section of the neovolcanic Pual Ridge. Fluid temperatures measured at the orifices of black or gray smokers and sulfide chimneys venting clear fluid range between 220°C and 276°C , and end-member vent fluids are acidic (pH 2.5–3.5), show high K/Ca ratios, and are high in Mn, Fe, and Pb relative to mid-ocean ridge fluids (Gamo et al., 1996; Shitashima et al., 1997; Douville, 1999). The fluids also exhibit variable salinities, which may imply subsurface phase separation, suggesting that hydrothermal temperatures exceed 350°C below the chimney fields. Douville et al. (1999) ascribe unusually high fluorine contents in the fluids to magmatic sources. Similarly, Ishibashi et al. (1996) explain end-member gas compositions of 20–40 mM CO_2 , 20–40 μM CH_4 , and $R/R_A(\text{He}) = 7.4$ by significant magmatic input into the hydrothermal fluids.

Drilling was attempted at the Satanic Mills site ($3^{\circ}43.63'\text{S}$, $151^{\circ}40.40'\text{E}$; 1708–1720 m water depth), the Roman Ruins site ($3^{\circ}43.27'\text{S}$, $151^{\circ}40.50'\text{E}$; 1693–1700 m water depth), and in an area of diffuse venting, the Snowcap site ($3^{\circ}43.67'\text{S}$, $151^{\circ}40.25'\text{E}$; 1654–1670 m water depth) (Binns, Barriga, Miller, et al., 2002). The Snowcap area is a site of extensive low-temperature (6°C) diffuse venting across a 10- to 15-m-high knoll with more intense activity at the edges. Dredge and submersible sampling recovered completely hydrothermally altered dacites dominated by advanced argillic alteration to cristobalite, with lesser natroalunite, diaspore, and illite-montmorillonite (Yeats et al., 2000).

We reported data for anhydrite from Snowcap (Site 1188) and Roman Ruins (Site 1189). Two holes were drilled at each site with maximum crustal penetrations of 375 meters below sea floor (mbsf) at Site 1188 and 200 mbsf at Site 1189. Rocks encountered in all drill holes are dacitic in composition and include massive to vesicular lava flows, autoclastic breccias, and volcanoclastic sediments. Except for fresh lava flows near the seafloor, all rocks are highly to completely altered to silica (cristobalite and quartz), clay (chlorite, illite, pyrophyllite, smectite, and mixed-layer phases), and anhydrite. X-ray diffraction (XRD) results indicate that the clay composition is variable with alternating illite- and chlorite-dominated assemblages in the shallow crust at PACMANUS. Thermal gradients at Site 1189 appear to be higher than those at Site 1188, as indicated by the shallower depth at which the transition from cristobalite to quartz occurs (30 vs. 120 mbsf) (Binns, Barriga, Miller, et al., 2002).

The common occurrence of anhydrite as vein and vesicle fill, but also replacive and as breccia cement, is remarkable. Anhydrite is typically associated with pyrite and, less frequently, with quartz. It appears to be generally late in the sequence of hydrothermal alteration stages, which

include early pervasive green clay-quartz alteration, localized quartz-white clay-anhydrite alteration, silicification, and late anhydrite-pyrite veining. Downhole profiles of mineral abundance suggest that the extent of silicification increases and the anhydrite contents decrease downsection in all drill holes (Binns, Barriga, Miller, et al., 2002). Moreover, relict igneous plagioclase (labradorite) is generally more abundant deeper in the sections, suggesting less intense alteration or conditions of fluid-rock reactions under which labradorite is stable.

Data are reported in Table T1 and plotted vs. depth in Figures F1, F2, and F3. This data report presents all anhydrite chemical data collected to this date. Subsets of this data collection were presented and discussed previously (Sr and S isotope compositions in Roberts et al. [2003]; REE data for Site 1188 in Bach et al. [2003]).

Figure F1 shows the downhole variability of Sr isotope compositions that vary between seawater (0.70918) (Palmer and Edmond, 1989) and an assumed hydrothermal end-member composition of 0.7050‰ (see discussions in Roberts et al., 2003, and Bach et al., 2003). At seawater salinity, anhydrite precipitates above 140–150°C when seawater is being heated or seawater (28 mmol/kg sulfate) mixes with nominally sulfate-free hydrothermal fluids. Sr concentrations in the PACMANUS black smoker fluids are slightly higher than those in seawater (Douville, 1999). A simple Sr mass balance provides the proportions of seawater in the fluids from which anhydrite was precipitated:

$$\% \text{seawater} = (R_{\text{HF}} \times C_{\text{HF}} - R_{\text{Anhy}} \times C_{\text{HF}}) / [R_{\text{HF}} \times C_{\text{HF}} - R_{\text{SW}} \times C_{\text{SW}} - R_{\text{Anhy}} \times (C_{\text{HF}} - C_{\text{SW}})] \times 100,$$

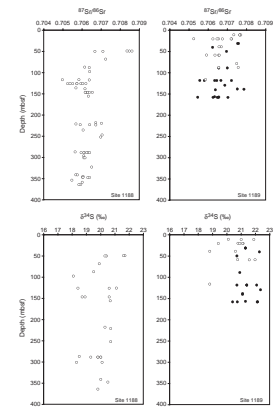
where $R = {}^{87}\text{Sr}/{}^{86}\text{Sr}$ ratio and $C = \text{Sr}$ concentration of seawater (SW), anhydrite (Anhy), and the hydrothermal fluid end-member (HF), respectively (Table T1).

The most radiogenic values (corresponding to 84%–89% seawater) were observed in the shallowest anhydrite veins cored in Hole 1188A. As discussed in Roberts et al. (2003) and Vanko et al. (2004), the formation of these veins requires some conductive heating of seawater for anhydrite saturation to be achieved in a mix that has >84% seawater. The average percent seawater for the PACMANUS anhydrites is $40\% \pm 17\%$ (1σ ; $n = 105$). By comparison, anhydrites recovered from drill core from the Trans-Atlantic Geotraverse (TAG) hydrothermal system at the Mid-Atlantic Ridge 26°N (Mills et al., 1998; Teagle et al., 1998a) precipitated from fluids with an average of $68\% \pm 12\%$ seawater (1σ ; $n = 42$). Anhydrite from Site 1189 yields an average of $47\% \pm 16\%$ seawater, which is somewhat higher than the average for anhydrite from Site 1188 ($35\% \pm 17\%$; $33\% \pm 13\%$ if the shallowest three samples are excepted).

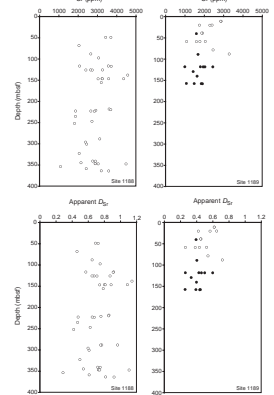
The sulfur isotopic composition of anhydrite from Site 1188 is mostly enriched in ${}^{32}\text{S}$ relative to seawater ($\delta^{34}\text{S} = 21\text{‰}$) (Rees et al., 1978). This could be due either to oxidation of sulfide or addition of sulfate derived from disproportionation of magmatic SO_2 (e.g., Gamo et al., 1997). $\delta^{34}\text{S}$ numbers of anhydrites from Hole 1189B and the majority of samples from Hole 1189A range between 20‰ and 23‰, similar to anhydrite from the TAG hydrothermal field (Chiba et al., 1998). As pointed out by Roberts et al. (2003), the $\delta^{34}\text{S}$ values of anhydrite from Site 1188 tend to be systematically lower by 1‰–2‰, which may relate to systematic differences in hydrothermal processes at these two sites.

T1. Chemical and isotopic compositions, p. 16.

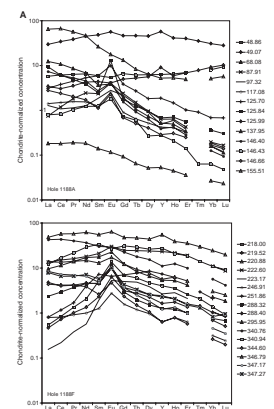
F1. Downhole variations in ${}^{87}\text{Sr}/{}^{86}\text{Sr}$ and $\delta^{34}\text{S}$ -CDT, p. 11.



F2. Downhole variations in Sr concentrations and apparent Sr distribution coefficients, p. 12.



F3. Chondrite-normalized rare earth element patterns, p. 13.



Sr concentrations of anhydrite are plotted vs. subbasement depth in Figure F2. Although there is some overlap, anhydrites from Site 1188 tend to have higher Sr concentrations than anhydrites from Site 1189. We used the Sr concentrations in combination with the calculated fraction of seawater to determine empirical Sr distribution coefficients:

$$D_{Sr} = (Sr/Ca)_{solid}/(Sr/Ca)_{fluid}.$$

The PACMANUS end-member hydrothermal fluid calculated by Bach et al. (2003) with data from Douville (1999) has higher Ca (20.1 mM) and Sr (0.114 mM) than seawater (Ca = 10.2 mM; Sr = 0.087 mM). The average calculated empirical Sr distribution coefficient for PACMANUS anhydrites is 0.62 ± 0.21 , basically identical to the D_{Sr} calculated by Teagle et al. (1998a) for anhydrites from the TAG hydrothermal field (0.62 ± 0.23) and a value of 0.67 provided by Kuhn et al. (2003) for anhydrite from the sediment-hosted Grimsey hydrothermal field north of Iceland. However, apparent D_{Sr} values seem to be greater for anhydrite from Site 1188 than for Site 1189 (Fig. F2). The average D_{Sr} for Site 1188 is 0.73 ± 0.18 , whereas that for Site 1189 is 0.46 ± 0.12 .

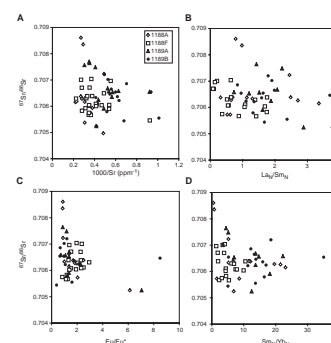
Chondrite-normalized REE diagrams (Fig. F3A, F3B) depict further discrepancies between anhydrites from Sites 1188 and 1189. Although anhydrites show uniform enrichment of light REE (La to Sm) at both sites, those with peculiar mid-REE (Sm to Dy) enrichments are limited to Site 1188. The overall variability in REE pattern shape and the range in total REE concentration appears greater among the samples from Site 1188. Bach et al. (2003) noted that the REE variability in anhydrite from PACMANUS is much greater than in anhydrites from TAG (Humphris, 1998) and suggested that this difference may indicate a more variable ligand chemistry in the PACMANUS fluids.

REE pattern shape and Sr isotope composition do not appear to be correlated in anhydrites (Fig. F4), indicating that the variations in the proportion of seawater in the fluid does not have a systematic impact on REE contents of anhydrite. In a diagram of $^{87}Sr/^{86}Sr$ vs. $1000/Sr$ (Fig. F4A), fluid mixing produces linear trends. Overall, the PACMANUS anhydrite data do not form a systematic trend in Figure F4A, indicating that processes other than fluid mixing have played a role.

SUMMARY

Sr and S isotope data and trace element data for anhydrite samples from drill core from the PACMANUS hydrothermal field reveal remarkable similarities and differences to anhydrite from the mid-ocean-ridge TAG system. A Sr mass balance indicates that, on average, there is less seawater present in the mixed fluids from which anhydrite precipitates. Within the PACMANUS area, the site of focused venting (Site 1189) appears to show more entrainment of seawater than the site of diffuse venting (Site 1188). Apparent distribution coefficients calculated for PACMANUS anhydrite are identical to those derived for anhydrite from TAG. Again, anhydrites from Site 1188 are distinct from those from Site 1189 and reveal higher apparent distribution coefficients. These differences are probably most pronounced in the $\delta^{34}S$ compositions that are dominantly $<21\text{‰}$ at Site 1188 and largely $>21\text{‰}$ at Site 1189. Rare earth element concentrations show a remarkable variability in PACMANUS anhydrites when compared to anhydrite from TAG. Most noteworthy is anhydrite with mid-REE enrichment from Site 1188. The

F4. $^{87}Sr/^{86}Sr$ ratios, p. 15.



differences in anhydrite geochemistry between PACMANUS and TAG and the differences between separate sites within the PACMANUS field can be used to infer contrasts in style and intensity of fluid flow and fluid-rock interaction.

ACKNOWLEDGMENTS

This grant used samples and/or data provided by the Ocean Drilling Program (ODP). ODP is sponsored by the U.S. National Science Foundation (NSF) and participating countries under management of Joint Oceanographic Institutions (JOI), Inc. Funding for this research was provided by JOI/US Science Support Program (USSSP) and NSF (grant number OCE0099106). Thanks to Jurek Blusztajn and Tracy Abbruzzese for conducting the Sr isotope analyses at WHOI, Lary Ball and Ed Sholkovitz for help with the REE and trace element analyses at WHOI, Brian Schroeder for help with the mineral separation, and Matthew Cooper for conducting Sr isotope and trace metal analyses at SOC. This paper represents WHOI contribution number 11192.

REFERENCES

- Bach, W., Roberts, S.R., Vanko, D.A., Binns, R.A., Yeats, C.J., Craddock, P.R., and Humphris, S.E., 2003. Controls of fluid chemistry and complexation on rare earth element contents of anhydrite from the PACMANUS subseafloor hydrothermal system, Manus Basin, Papua New Guinea. *Miner. Deposita*, 38:916–935.
- Bailey, S.A., and Smith, J.W., 1972. Improved method for the preparation of sulfur dioxide from barium sulfate for isotope ratio studies. *Anal. Chem.*, 44:1542–1543.
- Binns, R.A., Barriga, F.J.A.S., Miller, D.J., et al., 2002. *Proc. ODP, Init. Repts.*, 193 [CD-ROM]. Available from: Ocean Drilling Program, Texas A&M University, College Station TX 77845-9547, USA.
- Chiba, H., Uchiyama, N., and Teagle, D.A.H., 1998. Stable isotope study of anhydrite and sulfide minerals at the TAG hydrothermal mound, Mid-Atlantic Ridge, 26°N. In Herzig, P.M., Humphris, S.E., Miller, D.J., and Zierenberg, R.A. (Eds.), *Proc. ODP, Sci. Results*, 158: College Station, TX (Ocean Drilling Program), 85–90.
- Coggon, R.M., Teagle, D.A.H., Cooper, M.J., and Vanko, D.A., 2004. Linking basement carbonate vein compositions to porewater geochemistry across the eastern flank of the Juan de Fuca Ridge, ODP Leg 168. *Earth Planet. Sci. Lett.*, 219:111–128.
- Coleman, M.L., and Moore, M.P., 1978. Direct reduction of sulfates to sulfur dioxide for isotopic analysis. *Anal. Chem.*, 50:1594–1595.
- Douville, E. 1999. Les fluides hydrothermaux oceaniques comportement geochimique des elements traces et des terres rares: processus associes et modelisation thermodynamique [Ph.D. Thesis]. Univ. Brest, France.
- Douville, E., Bienvenu, P., Charlou, J.L., Donval, J.P., Fouquet, Y., Appriou, P., and Gamo, T., 1999. Yttrium and rare earth elements in fluids from various deep-sea hydrothermal systems. *Geochim. Cosmochim. Acta*, 63:627–643.
- Gamo, T., Okamura, K., Charlou, C.L., Urabe, T., Auzende, J.-M., Ishibashi, J., Shitashima, K., Chiba, H., and ManusFlux Shipboard Science Party, 1997. Acidic and sulfate-rich hydrothermal fluids from the Manus back-arc basin, Papua New Guinea. *Geology*, 25:139–142.
- Gamo, T., Okamura, K., Kodama, Y., Charlou, J.-L., Urabe, T., Auzende, J.-M., Shipboard Scientific Party of the ManusFlux Cruise, and Ishibashi, J., 1996. Chemical characteristics of hydrothermal fluids from the Manus back-arc basin, Papua New Guinea, I. Major chemical components. *Eos, Trans. Am. Geophys. Union*, 77:W116. (Abstract)
- Humphris, S.E., 1998. Rare earth element composition of anhydrite: implications for deposition and mobility within the active TAG hydrothermal mound. In Herzig, P.M., Humphris, S.E., Miller, D.J., and Zierenberg, R.A. (Eds.), *Proc. ODP, Sci. Results*, 158: College Station, TX (Ocean Drilling Program), 143–159.
- Ishibashi, J., Wakita, H., Okamura, K., Gamo, T., Shitashima, K., Charlou, J.L., Jean-Baptiste, P., and Shipboard Party, 1996. Chemical characteristics of hydrothermal fluids from the Manus back-arc basin, Papua New Guinea, II. Gas components. *Eos, Trans. Am. Geophys. Union*, 77:W116. (Abstract)
- Kuhn, T., Herzig, P.M., Hannington, M.D., Garbe-Schönberg, D., and Stoffers, P., 2003. Origin of fluids and anhydrite precipitation in the sediment-hosted Grimsey hydrothermal field north of Iceland. *Chem. Geol.*, 202:5–21.
- Mills, R.A., and Elderfield, H., 1995. Rare earth element geochemistry of hydrothermal deposits from the active TAG mound, 26°N Mid-Atlantic Ridge. *Geochim. Cosmochim. Acta*, 59:3511–3524.
- Mills, R.A., Teagle, D.A.H., and Tivey, M.K., 1998. Fluid mixing and anhydrite precipitation within the TAG mound. In Herzig, P.M., Humphris, S.E., Miller, D.J., and Zierenberg, R.A. (Eds.), *Proc. ODP, Sci. Results*, 158: College Station, TX (Ocean Drilling Program), 119–127.

- Mills, R.A., and Tivey, M.K., 1999. Seawater entrainment and fluid evolution within the TAG hydrothermal mound: evidence from analyses of anhydrite. *In* Cann, J., Elderfield, H., and Laughton, A. (Eds.), *Mid-Ocean Ridges: Dynamics of Processes Associated with the Creation of New Ocean Crust*: Cambridge (Cambridge Univ. Press), 225–248.
- Palmer, M.R., and Edmond, J.M., 1989. The strontium isotope budget of the modern ocean. *Earth Planet. Sci. Lett.*, 92:11–26.
- Paulick, H., Vanko, D.A., and Yeats, C.J., 2004. Drill core-based facies reconstruction of a deep-marine felsic volcano hosting an active hydrothermal system (Pual Ridge, Papua New Guinea, ODP Leg 193). *J. Volcanol. Geotherm. Res.*, 130:31–50.
- Rees, C.W., Jenkins, W.J., and Monster, J., 1978. The sulfur isotope geochemistry of ocean water sulfate. *Geochim. Cosmochim. Acta*, 42:377–382.
- Roberts, R., Bach, W., Binns, R.A., Vanko, D.A., Yeats, C.J., Teagle, D.A.H., Blacklock, K., Blusztajn, J.S., Boyce, A.J., Cooper, M.J., Holland, N., and McDonald, B., 2003. Contrasting evolution of hydrothermal fluids in the PACMANUS system, Manus Basin: the Sr and S isotope evidence. *Geology*, 31(9):805–808.
- Shitashima, K., Gamo, T., Okamura, K., and Ishibashi, J., 1997. Trace elements at the Manus Basin, Papua New Guinea. *JAMSTEC J. Deep Sea Res.*, 13:249–255.
- Sun, S.-S., and McDonough, W.F., 1989. Chemical and isotopic systematics of oceanic basalts: implications for mantle composition and processes. *In* Saunders, A.D., and Norry, M.J. (Eds.), *Magmatism in the Ocean Basins*. Geol. Soc. Spec. Publ., 42:313–345.
- Teagle, D.A.H., Alt, J.C., Chiba, H., Humphris, S.E., and Halliday, A.N., 1998a. Strontium and oxygen isotopic constraints on fluid mixing, alteration and mineralization in the TAG hydrothermal deposit. *Chem. Geol.*, 149:1–24.
- Teagle, D.A.H., Alt, J.C., and Halliday, A.N., 1998b. Tracing the chemical evolution of fluids during hydrothermal recharge: constraints from anhydrite recovered in ODP Hole 504B. *Earth Planet. Sci. Lett.*, 155:167–182.
- Vanko, D.A., Bach, W., Roberts, S., Yeats, C.J., and Scott, S.D., 2004. Fluid inclusion evidence for subsurface phase separation and variable fluid mixing regimes beneath the deep-sea PACMANUS hydrothermal field, Manus Basin back arc rift, Papua New Guinea. *J. Geophys. Res.*, 109(B3):10.1029/2003JB002579.
- Yeats, C.J., Binns, R.A., and Parr, J.M., 2000. Advanced argillic alteration associated with actively forming, submarine polymetallic sulfide mineralisation in the eastern Manus Basin, Papua New Guinea. *Geol. Soc. Aust.*, 59:555. (Abstract)

Figure F1. Downhole variations in $^{87}\text{Sr}/^{86}\text{Sr}$ and $\delta^{34}\text{S}$ (V-CDT) of anhydrite at Site 1188 (Holes 1188A from 0 to 218 mbsf and Hole 1188F from 230 to 375 mbsf) and Site 1189 (open symbols = Hole 1189A; solid symbols = Hole 1189B).

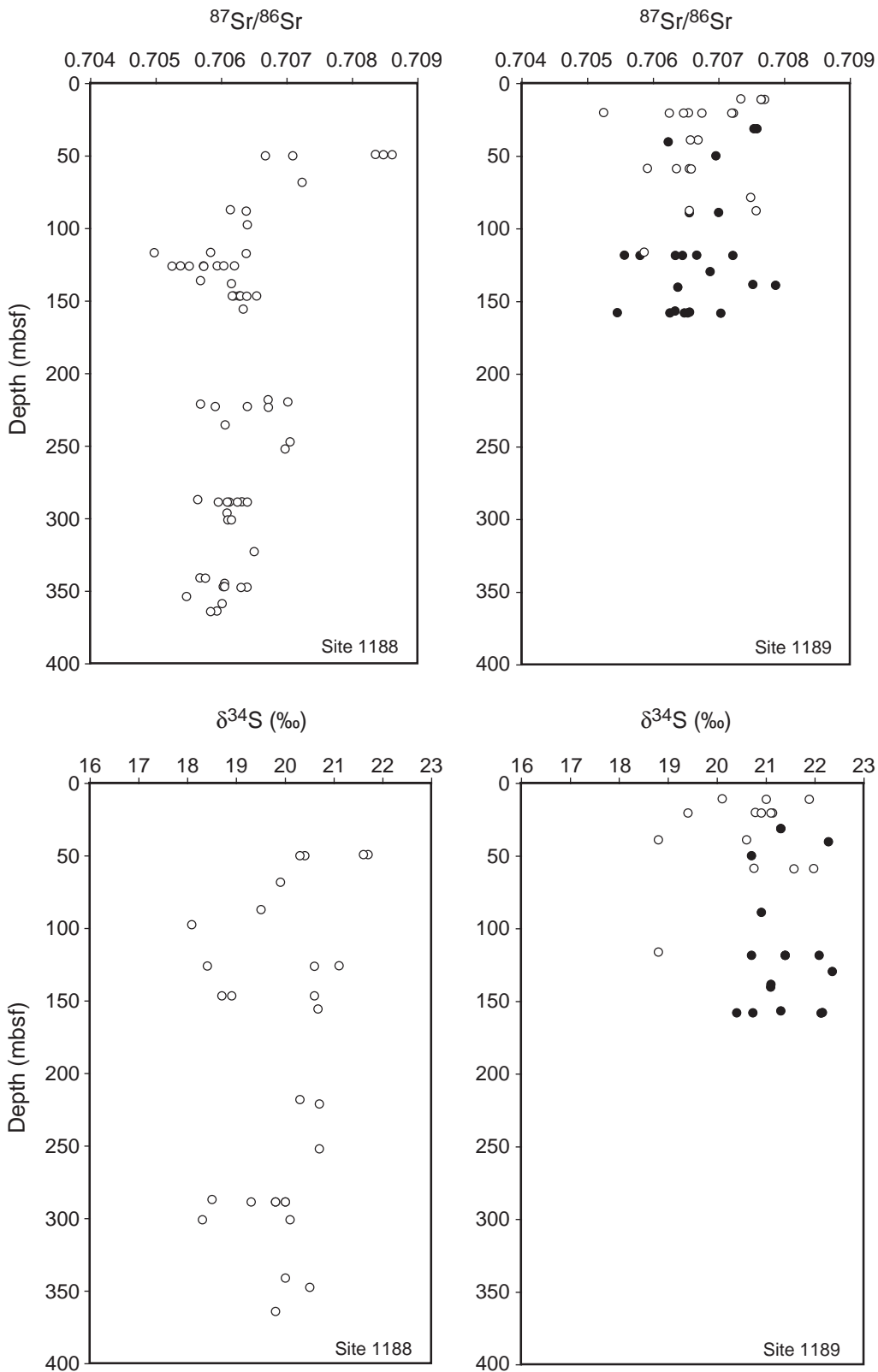


Figure F2. Downhole variations in Sr concentrations and apparent Sr distribution coefficients (see text) of anhydrite at Sites 1188 (Holes 1188A and 1188F) and 1189 (open symbols = Hole 1189A; solid symbols = Hole 1189B).

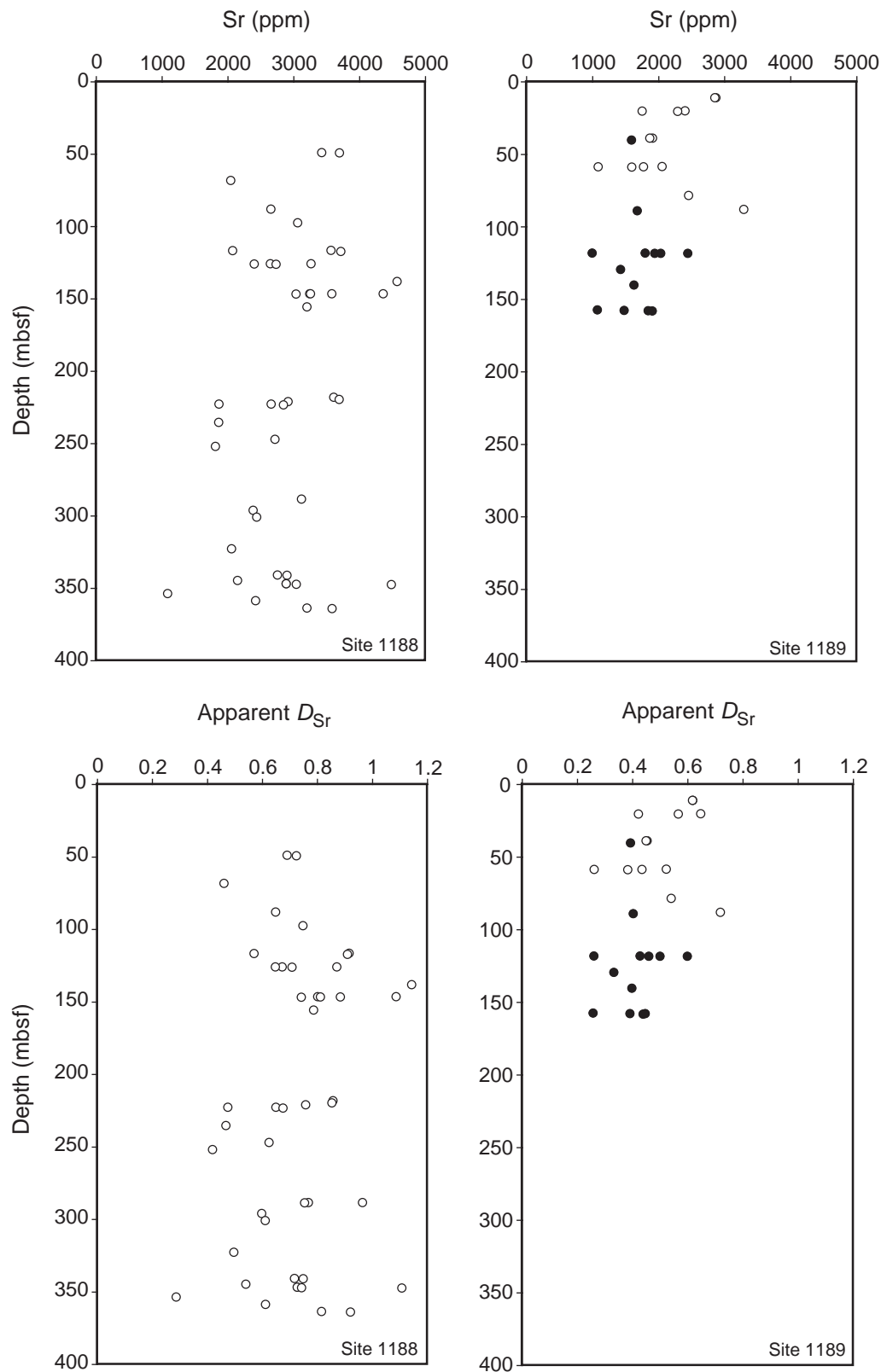


Figure F3. A. Chondrite-normalized rare earth element patterns of anhydrite from Site 1188. Note that data that were produced at WHOI lack Tm because it was used as an internal standard in the ICP-MS procedure. The subbasement depths of the samples are used as identifiers (cf. Table T1, p. 16). Chondrite concentrations are from Sun and McDonough (1989). (Continued on next page.)

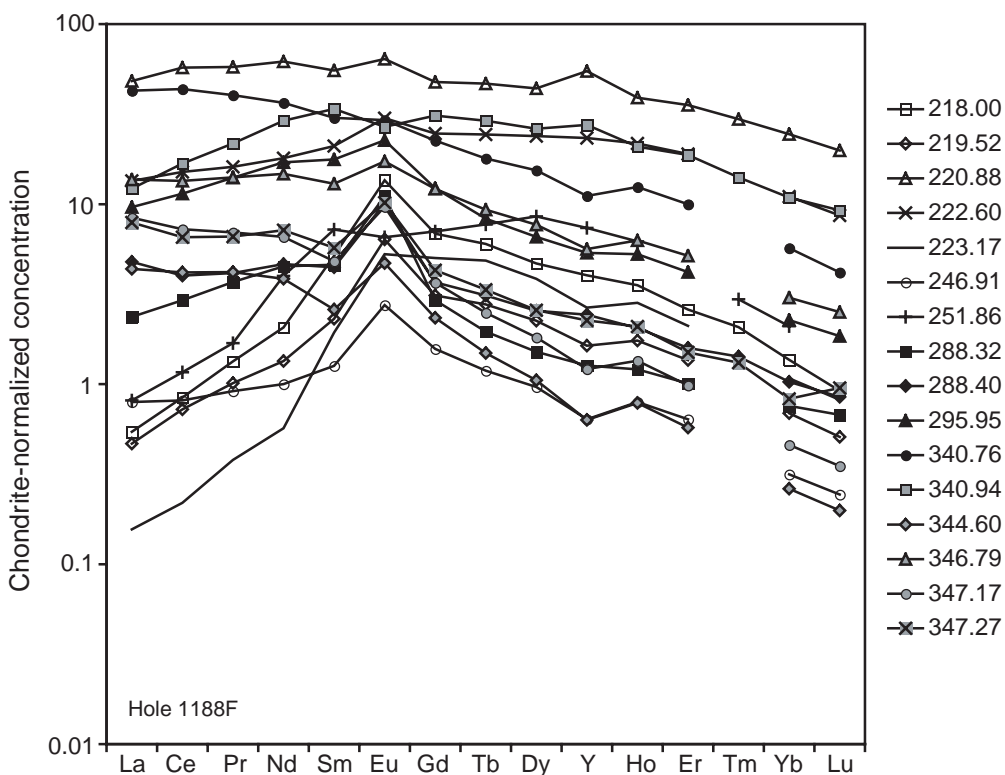
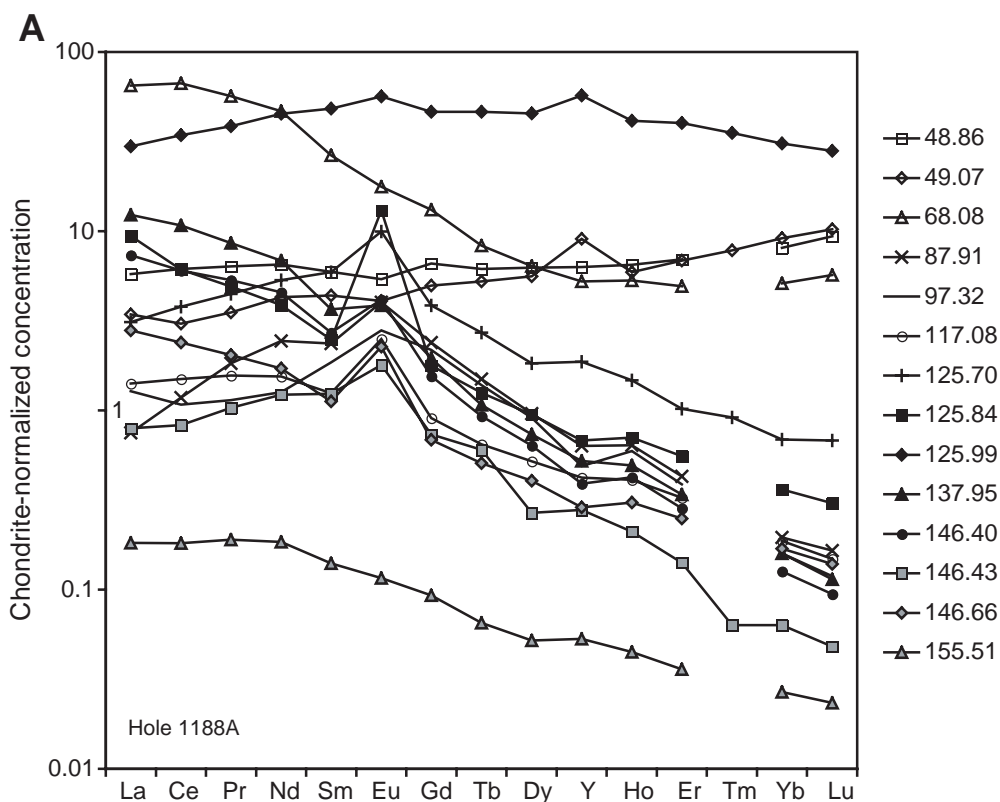


Figure F3 (continued). B. Chondrite-normalized rare earth element patterns of anhydrite from Site 1189.

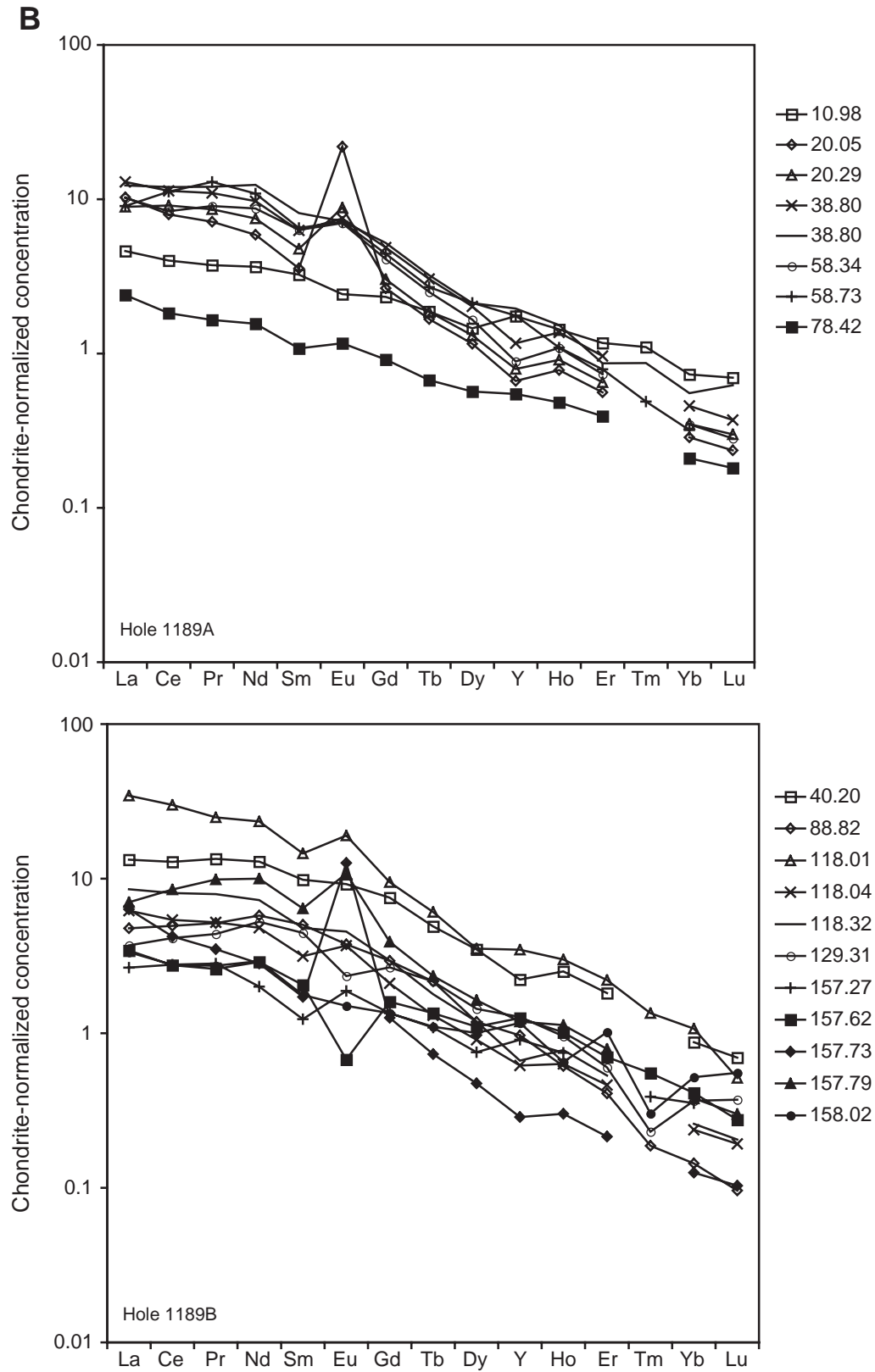


Figure F4. $^{87}\text{Sr}/^{86}\text{Sr}$ ratios of anhydrite plotted against (A) inverse Sr concentrations, (B) chondrite-normalized La/Sm ratios, (C) chondrite-normalized Eu anomaly [$\text{Eu}_\text{N}/(\text{Sm}_\text{N}+\text{Gd}_\text{N})/2$], and (D) chondrite-normalized Sm/Yb ratios.

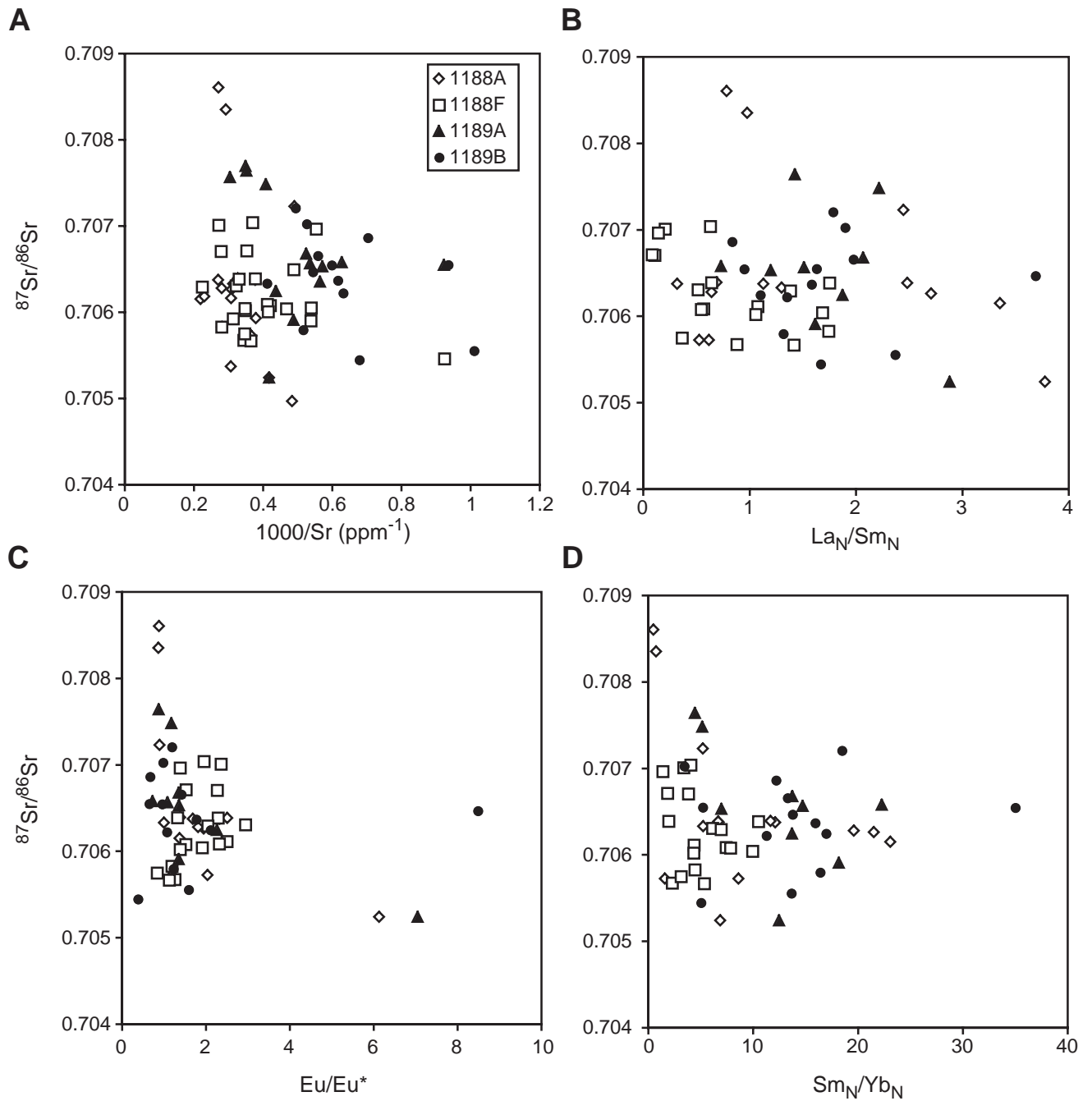


Table T1. Chemical and isotopic compositions (ppm) of anhydrite separates from hydrothermal veins and vug fills. (Continued on next seven pages.)

Laboratory:	WHOI	CSIRO	SOC	CSIRO	CSIRO	WHOI	CSIRO	WHOI	WHOI/SOC	WHOI	WHOI	WHOI	SOC
Hole:	1188A												
Core, section:	7R-1	7R-1	7R-1	7R-2	7R-2	9R-1	11R-1	11R-1	12R-1	14R-1	14R-1	14R-1	15R-1
Piece, interval (cm):	12, 66–68	13, 80–82	14, 87–89	1, 17–21	1, 17–21	6, 48–52	2, 15–20	8, 101–107	7, 72–74	7, 47–50	10, 66–70	15, 108–110	1, 0–2
Depth (mbsf):	48.86	49.00	49.07	49.87	49.87	68.08	87.05	87.91	97.32	116.47	116.66	117.08	125.70
Description:	Drusy anhy vein, subhorizontal	Anhy vein (2–5 mm), subhorizontal	Anhy-py vein (2–8 mm), subhorizontal	Coarse anhy vein, late	Earlier network of thin anhy veins	Anhy vein with bleached halo	Anhy vein; bleached halo	Anhy-py vein; bleached halo	Thick anhy vein; bleached halo	Narrow anhy veins; silicified halos	Narrow anhy veins; silicified halos	Breccia cement	Crustiform anhy (≤3 mm) in vein >1 cm
⁸⁷ Sr/ ⁸⁶ Sr	0.708352	0.708471	0.708606	0.707086	0.706668	0.707230	0.706135	0.706377	0.706394	0.705831	0.704970	0.706377	0.705725
δ ³⁴ S V-CDT (‰)		21.7	21.6	20.4	20.3	19.9	19.5		18.1				21.1
% seawater	84.1	86.5	89.2	56.6	46.5	60.0	32.8	39.2	39.6	24.5	–0.9	39.2	21.6
Sr	3425		3693			2041		2651	3057	3563	2070	3712	
D (Ca-Sr)	0.689		0.723			0.460		0.648	0.747	0.915	0.570	0.909	
Mg			9										9
Li	0.483					0.5207		1.1707	0.149			0.209	
Rb	0.049		0.048			0.166		0.033	0.247			0.042	0.048
Cs	0.003		0.001			0.017		0.007	0.020			0.006	0.002
Ba	10.59		32.42			33.44		21.91	10.89			5.19	36.36
La	1.369		0.812			15.383		0.178	0.303			0.334	0.738
Ce	3.774		1.865			40.827		0.721	0.658			0.916	2.315
Pr	0.604		0.335			5.389		0.174	0.108			0.149	0.424
Nd	2.982		1.963			21.384		1.114	0.579			0.708	2.437
Sm	0.906		0.670			4.062		0.362	0.284			0.191	0.905
Eu	0.313		0.237			1.027		0.233	0.162			0.145	0.577
Gd	1.355		1.020			2.710		0.491	0.448			0.186	0.792
Tb	0.231		0.196			0.311		0.056	0.052			0.024	0.102
Dy	1.589		1.424			1.620		0.244	0.231			0.132	0.464
Ho	0.367		0.335			0.301		0.036	0.034			0.023	0.083
Er	1.154		1.136			0.814		0.071	0.064			0.054	0.169
Tm			0.200										0.023
Yb	1.374		1.554			0.871		0.033	0.027			0.032	0.117
Lu	0.237		0.260			0.144		0.004	0.003			0.004	0.017
Y	9.89		14.22			8.25		0.99	0.77			0.66	2.93
Pb	1.42		0.17			9.16		0.14	1.19			1.01	9.80
U	0.007		0.002			0.025		0.004	0.012			0.002	n.d.
P	13.7					120.9		674.8	144.9			242.6	
As	0.05					0.70		0.14	0.05			0.05	
La/Sm	0.98		0.78			2.44		0.32	0.69			1.13	0.53
Sm/Yb	0.73		0.48			5.18		12.09	11.65			6.70	8.59
La/Yb	0.71		0.40			12.67		3.83	8.01			7.57	14.67
Eu/Eu*	0.86		0.87			0.89		1.69	1.38			2.32	2.04

Notes: WHOI = Woods Hole Oceanographic Institution (USA), CSIRO = Commonwealth Scientific and Industrial Research Organisation (Australia), SOC = Southampton Oceanography Centre (UK). Anhy = anhydrite, py = pyrite, qtz = quartz, gyp = gypsum, mt = magnetite, volc = volcanics. Fg = fine grained. ND = not determined.

Table T1 (continued).

Laboratory:	WHOI	Sr duplicate	CSIRO	CSIRO	WHOI	SOC	CSIRO	CSIRO	WHOI	WHOI	Sr duplicate	SOC
Hole:	1188A											
Core, section:	15R-1	15R-1	15R-1	15R-1	15R-1	15R-1	16R-1	15R-1	16R-2	17R-1	17R-1	17R-1
Piece, interval (cm):	2, 5-9	2, 5-9	2, 5-7	3, 10-11	4, 14-20	7, 29-31	8, 47-50	2, 5-7	15, 109-111	23, 130-133	23, 130-133	24, 133-136
Depth (mbsf):	125.75	125.75	125.75	125.80	125.84	125.99	135.87	125.75	137.95	146.40	146.40	146.43
Description:	Crustiform anhy vein; mainly bladed crystals	Crustiform anhy vein; mainly bladed crystals	Bladed zone of multiple anhy vein; younger?	Coarse granular anhy (snowball)	Crustiform anhy vein	Anhy from 2-mm vein selvage; bleached volc	Granular anhy in vein jog	Granular zone of multiple veins; older?	Anhy-mt-py vein	Anhy-mt-py vein	Anhy-mt-py vein	Anhy-mt-py vein
⁸⁷ Sr/ ⁸⁶ Sr	0.705371	0.705933	0.706195	0.705508	0.705241	0.705726	0.705677	0.706032	0.706152	0.706265	0.706183	0.706281
δ ³⁴ S V-CDT (‰)				18.4		20.6						20.6
% seawater	11.3	27.4	34.4	15.3	7.4	21.6	20.2	30.0	33.3	36.3	34.1	36.7
Sr	3262	2642			2400	2731			4568	3239	4355	3575
D (Ca-Sr)	0.870	0.672			0.646	0.707			1.143	0.801	1.086	0.883
Mg						225						137
Li					0.132				0.494	0.381		
Rb					0.139	0.301			0.450	0.329		0.286
Cs					0.007	0.012			0.022	0.008		0.005
Ba					141.08	90.12			19.01	21.97		26.09
La					2.224	7.046			2.917	1.743		0.188
Ce					3.738	21.002			6.591	3.685		0.507
Pr					0.466	3.656			0.817	0.505		0.098
Nd					1.766	20.642			3.129	2.086		0.560
Sm					0.380	7.388			0.562	0.416		0.190
Eu					0.757	3.279			0.223	0.241		0.104
Gd					0.365	9.538			0.401	0.319		0.151
Tb					0.047	1.737			0.040	0.035		0.023
Dy					0.241	11.541			0.186	0.162		0.068
Ho					0.040	2.336			0.028	0.024		0.012
Er					0.092	6.653			0.056	0.047		0.023
Tm						0.903						0.002
Yb					0.062	5.245			0.027	0.021		0.011
Lu					0.008	0.712			0.003	0.002		0.001
Y					1.07	89.63			0.82	0.61		0.44
Pb					0.07	1.34			0.89	2.31		0.27
U					0.007	0.044			0.007	0.008		0.009
P					106.8				175.8	162.3		
As					0.13				0.13	0.24		
La/Sm					3.78	0.62			3.35	2.71		0.64
Sm/Yb					6.86	1.57			23.07	21.50		19.59
La/Yb					25.91	2.02			77.33	58.18		37.21
Eu/Eu*					6.13	1.19			1.37	1.95		1.81

Table T1 (continued).

Laboratory:	CSIRO	CSIRO	WHOI	WHOI	WHOI/SOC	SOC	WHOI	SOC	WHOI	Sr duplicate	WHOI	WHOI	WHOI
Hole:	17R-1		17R-1		17R-1		17R-1		17R-1		1188F		
Core, section:	17R-1	17R-1	17R-1	17R-1	18R-1	1Z-1	1Z-2	1Z-3	1Z-4	1Z-4	3Z-1	7Z-1	14Z-1
Piece, interval (cm):	24, 137-140	24, 137-140	25, 140-142	2, 6-9	19, 81-84	1, 0-2	2, 32-34	2, 48-50	2, 100-104	2, 100-104	1C, 57-61	1C, 30-36	6, 101-105
Depth (mbsf):	146.47	146.47	146.50	146.66	155.51	218.00	219.52	220.88	222.60	222.60	223.17	235.30	246.91
Description:	Late drusy anhy vein	Early, thin, bladed anhy-(gyp) vein	Anhy- <i>mt</i> - <i>py</i> vein	Anhy empty vein	Coarse-grained anhy + <i>py</i> vug fill	<i>Py</i> -anhy vein	Anhy- <i>py</i> - <i>qtz</i> veins; cyclic halos	Crustiform anhy in 5-mm anhy vein	Anhy- <i>py</i> - <i>qtz</i> veins; cyclic halos	Thick anhy- <i>py</i> veins; complex halos			
⁸⁷ Sr/ ⁸⁶ Sr	0.706289	0.706534	0.706165	0.706387	0.706331	0.706710	0.707012	0.705679	0.706393	0.705904	0.706717	0.706056	0.707044
$\delta^{34}\text{S}$ V-CDT (‰)	18.7	18.9			20.7	20.3		20.7					
% seawater	36.9	43.2	33.6	39.4	38.0	47.6	54.9	20.3	39.6	26.6	47.7	30.7	55.6
Sr			3252	3033	3197	3604	3690	2913	2657	1862	2844	1859	2715
D (Ca-Sr)			0.811	0.741	0.786	0.856	0.852	0.757	0.649	0.474	0.674	0.467	0.624
Mg						75		7					
Li				0.14	0.155		0.403		0.087		0.195		0.042
Rb				0.021	0.059	0.116	0.110	0.078	0.088		0.094		0.201
Cs				0.001	0.019	0.011	0.016	0.000	0.007		0.004		0.005
Ba				5.42	5.65	40.43	46.58	19.49	45.66		278.14		26.82
La				0.661	0.043	0.129	0.111	11.457	3.192		0.037		0.188
Ce				1.464	0.111	0.516	0.442	35.069	9.220		0.134		0.497
Pr				0.193	0.018	0.127	0.096	5.489	1.532		0.036		0.087
Nd				0.783	0.084	0.944	0.613	28.282	8.211		0.260		0.456
Sm				0.172	0.021	0.790	0.353	8.440	3.223		0.295		0.193
Eu				0.131	0.007	0.788	0.369	3.715	1.739		0.305		0.159
Gd				0.141	0.019	1.409	0.640	9.793	5.069		1.032		0.322
Tb				0.019	0.002	0.225	0.103	1.749	0.910		0.182		0.044
Dy				0.103	0.013	1.190	0.570	11.135	6.072		0.979		0.245
Ho				0.017	0.003	0.201	0.099	2.207	1.230		0.160		0.045
Er				0.041	0.006	0.430	0.225	5.879	3.142		0.348		0.106
Tm						0.053		0.756					
Yb				0.029	0.005	0.232	0.117	4.159	1.873		0.183		0.054
Lu				0.004	0.001	0.023	0.013	0.505	0.219		0.021		0.006
Y				0.45	0.08	6.32	2.57	85.84	36.52		4.17		1.00
Pb				0.15	0.11	0.39	0.83	1.55	0.91		0.42		5.02
U				0.006	0.002	0.007	0.003	0.017	0.004		0.004		0.005
P				178.7	98.1		159.8		81.2		987.8		170.2
As				0.05	0.06		0.15		0.09		0.45		0.11
La/Sm				2.48	1.30	0.11	0.20	0.88	0.64		0.08		0.63
Sm/Yb				6.65	5.22	3.79	3.34	2.26	1.91		1.79		4.00
La/Yb				16.51	6.79	14.81	0.68	3.22	1.22		0.14		2.51
Eu/Eu*				2.51	1.00	2.26	2.35	1.25	1.31		1.51		1.94

Table T1 (continued).

Laboratory:	WHOI/SOC	CSIRO	WHOI	SOC	SOC	CSIRO	CSIRO	CSIRO	WHOI	WHOI/SOC	CSIRO	WHOI	WHOI
Hole:	1188F												
Core, section:	15Z-1	23Z-1	23Z-2	23Z-2	23Z-2	23Z-2	23Z-2	23Z-2	25Z-1	26Z-1	26Z-1	31Z-1	35Z-1
Piece, interval (cm):	16, 146-149	3, 15-19	2, 22-26	3B, 30-33	3C, 34-36	3C, 37-40	3C, 37-40	3C, 37-40	5, 35-40	4, 62-69	4, 62-64	1, 9-12	2E, 76-79
Depth (mbsf):	251.86	286.75	288.32	288.40	288.44	288.47	288.47	288.47	295.95	300.72	300.72	322.69	340.76
Description:	Anhy vein (1-2 mm)	Coarse anhy-py vein; zoned halo	Anhy-py vein; complex halos	Anhy from 2-mm vein	Fg anhy from 3-mm anhy vein; multiple events	Younger vein; older layer?	Younger vein; younger layer?	Older vein	Anhy-py veins cut by anhy vein	Anhy-mt-py veins	Thick vein; bleached halo	Anhy vein	Anhy-py vein
⁸⁷ Sr/ ⁸⁶ Sr	0.706969	0.705634	0.706310	0.706116	0.706089	0.706396	0.706242	0.705949	0.706083	0.706095	0.706150	0.706498	0.705671
$\delta^{34}\text{S V-CDT}$ (‰)	20.7	18.5		19.8	20.0	19.3	20.0	19.8		18.3	20.1		
% seawater	53.9	19.0	37.4	32.3	31.6	39.7	35.6	27.8	31.4	31.7	33.2	42.3	20.0
Sr	1810		3116	3842	3002				2381	2435		2052	2753
D (Ca-Sr)	0.418		0.767	0.963	0.753				0.597	0.610		0.496	0.716
Mg				47	42								
Li	0.257		0.328						0.074				0.942
Rb	0.092		0.273	0.216	0.156				0.181				0.340
Cs	0.026		0.023	0.008	0.002				0.011				0.029
Ba	20.95		20.00	39.25	41.96				20.27				62.47
La	0.131		0.560	1.132	0.636				2.281				10.108
Ce	0.496		1.787	2.450	1.743				6.981				26.632
Pr	0.110		0.351	0.393	0.355				1.333				3.828
Nd	0.773		2.065	2.124	2.139				7.790				16.686
Sm	0.610		0.705	0.681	0.728				2.712				4.620
Eu	0.419		0.640	0.587	0.532				1.311				1.701
Gd	1.343		0.600	0.755	0.657				2.516				4.632
Tb	0.263		0.073	0.116	0.083				0.310				0.669
Dy	1.955		0.385	0.649	0.439				1.671				3.912
Ho	0.417		0.068	0.116	0.079				0.298				0.704
Er	1.026		0.167	0.263	0.170				0.695				1.650
Tm				0.036	0.022								
Yb	0.503		0.129	0.175	0.110				0.386				0.968
Lu	0.053		0.017	0.022	0.014				0.047				0.106
Y	13.42		1.99	3.82	2.79				8.40				17.42
Pb	2.59		0.28	0.25	0.13				1.42				0.75
U	0.003		0.002	0.010	0.005				0.003				0.007
P	351.4		519.7						98.3				325.7
As	0.08		0.15						0.18				0.07
La/Sm	0.14		0.51	1.07	0.56				0.54				1.41
Sm/Yb	1.35		6.09	4.33	7.39				7.81				5.30
La/Yb	0.19		3.12	11.90	16.91				4.24				7.49
Eu/Eu*	1.37		2.93	2.49	2.31				1.51				1.11

Table T1 (continued).

Laboratory:	SOC	WHOI	WHOI	Sr dup	WHOI	SOC	WHOI	WHOI	WHOI	SOC	CSIRO	WHOI	CSIRO
Hole:	1188F												
Core, section:	35Z-1	37Z-1	37Z-2	37Z-2	37Z-2	37Z-2	39Z-1	40Z-1	41Z-1	41Z-1	2R-1	1189A	2R-1
Piece, interval (cm):	2H, 94-99	1, 10-14	7, 98-104	7, 98-104	9, 135-140	9, 145-147	1, 0-3	2F, 55-60	4A, 100-102	5, 137-138	14,	15, 114-116	16, 117-120
Depth (mbsf):	340.94	344.60	346.79	346.79	347.17	347.27	353.50	358.55	363.50	363.87	10.63	10.84	10.87
Description:	Anhy selvage (2 mm) on bleached volc	Anhy-py vein	Anhy-py vein	Anhy-py vein	Anhy-py vein	Anhy vein (5 mm)	Anhy-py vein	Anhy-py vug	Anhy-py vug	Anhy vein	Breccia matrix	Breccia matrix	Breccia matrix
⁸⁷ Sr/ ⁸⁶ Sr	0.705753	0.706045	0.706025	0.706047	0.706389	0.706296	0.705464	0.706009	0.705929	0.705832	0.707330	0.707695	0.707644
$\delta^{34}\text{S}$ V-CDT (‰)	20.0					20.5				19.8	20.1	21.0	
% seawater	22.4	30.4	29.9	30.5	39.5	37.1	14.1	29.4	27.2	24.6	62.3	70.4	69.3
Sr	2897	2145	2883	2885	3038	4483	1083	2418	3199	3581		2868	
D (Ca-Sr)	0.748	0.540	0.727	0.727	0.742	1.107	0.286	0.611	0.814	0.920		0.618	
Mg	21					228				14			
Li		0.163	0.117		0.16								
Rb	0.369	0.142	0.278		0.101	0.137				0.410			
Cs	0.007	0.003	0.006		0.006	0.001							
Ba	48.95	44.93	20.28		27.59	41.43				75.40			
La	2.894	1.033	3.238		1.993	1.870				8.698			
Ce	10.283	2.552	8.240		4.436	4.014				19.774			
Pr	2.066	0.398	1.337		0.662	0.627				2.779			
Nd	13.257	1.759	6.721		3.006	3.271				13.443			
Sm	5.162	0.397	1.982		0.736	0.874				3.226			
Eu	1.561	0.272	1.001		0.560	0.591				1.303			
Gd	6.379	0.480	2.494		0.752	0.881				3.481			
Tb	1.085	0.056	0.348		0.093	0.125				0.556			
Dy	6.659	0.267	1.953		0.462	0.654				2.990			
Ho	1.180	0.044	0.356		0.076	0.118				0.580			
Er	3.102	0.095	0.856		0.163	0.249				1.424			
Tm	0.358					0.034				0.175			
Yb	1.851	0.045	0.513		0.078	0.141				0.813			
Lu	0.235	0.005	0.064		0.009	0.024				0.104			
Y	43.23	0.99	8.82		1.91	3.55				17.84			
Pb	0.31	1.84	0.71		13.15	40.22				0.89			
U	0.004	0.003	0.004		0.003	0.008				<0.001			
P		111.5	177.4		123.3								
As		0.06	0.12		0.10								
La/Sm	0.36	1.68	1.05		1.75	1.38				1.74			
Sm/Yb	3.10	9.91	4.30		10.47	6.90				4.41			
La/Yb	2.91	16.65	4.53		18.32	10.72				5.48			
Eu/Eu*	0.83	1.90	1.38		2.28	2.04				1.18			

Table T1 (continued).

Laboratory:	SOC	WHOI/SOC	SOC	WHOI/SOC	CSIRO	CSIRO	CSIRO	CSIRO	WHOI/SOC	SOC	WHOI/SOC	WHOI/SOC	WHOI	SOC
Hole:	1189A													
Core, section:	2R-1	3R-1	3R-1	3R-1	3R-1	3R-1	3R-1	3R-1	5R-1	5R-1	7R-1	7R-1	7R-1	7R-1
Piece, interval (cm):	17, 128–129	11, 65–68	14, 81–83	16, 89–93	16, 89–93	16, 89–93	16, 89–93	16, 89–93	1, 0–3	1, 0–3	2, 4–8	3, 19–23	4, 24–26	6, 43–46
Depth (mbsf):	10.98	20.05	20.21	20.29	20.29	20.29	20.29	20.29	38.80	38.80	58.34	58.49	58.54	58.73
Description:	Breccia matrix	Crustiform anhy + py vein selvage	Crustiform anhy + py vein selvage	Banded anhy-py vein (cockade structure)	Zone A, coarse white	Zone B gray; oldest?	Zone C, bladed, white crystals	Zone D, gray; youngest?	Anhy vein	Thin (<1 mm) anhy vein	Anhy vein	Center of anhy vein	Anhy vein	Anhy vein
⁸⁷ Sr/ ⁸⁶ Sr	0.707642	0.705241	0.706534	0.706245	0.706739	0.706459	0.707220	0.707194	0.706680	0.706565	0.705910	0.706548	0.706354	0.706579
δ ³⁴ S V-CDT (‰)	21.9	20.8		21.1	20.9		19.4	21.1	20.6	18.8	20.8	22.0		21.6
% seawater	69.2	7.4	43.2	35.7	48.3	41.3	59.7	59.1	46.8	44.0	26.7	43.5	38.6	44.3
Sr	2848	2400	1750	2289					1907	1867	2050	1084	1771	1593
D(Ca-Sr)	0.617	0.646	0.421	0.566					0.453	0.448	0.522	0.260	0.433	0.382
Mg	45		82							464				429
Li		0.183		0.241					0.061		0.078			
Rb	0.022	0.072	0.141	0.076					0.175	0.156	0.105			0.081
Cs	0.001	0.014		0.008					0.005	0.001	0.004			0.004
Ba	19.46	17.82	55.80	38.88					29.64	57.44	54.33			36.18
La	1.095	2.437	2.174	2.119					3.071	2.916	2.422			1.879
Ce	2.452	4.872	6.015	5.567					6.945	7.339	5.113			5.536
Pr	0.355	0.680	1.002	0.817					1.042	1.142	0.858			1.063
Nd	1.669	2.693	5.063	3.433					4.446	5.659	3.987			5.930
Sm	0.496	0.546	1.173	0.731					0.960	1.246	0.967			1.663
Eu	0.141	1.270	0.535	0.512					0.434	0.418	0.407			0.377
Gd	0.478	0.544	1.222	0.623					0.999	1.071	0.840			1.467
Tb	0.070	0.062	0.125	0.070					0.114	0.121	0.094			0.166
Dy	0.369	0.293	0.776	0.334					0.513	0.539	0.421			0.685
Ho	0.081	0.044	0.140	0.051					0.078	0.087	0.062			0.100
Er	0.194	0.093	0.295	0.108					0.160	0.143	0.122			0.181
Tm	0.028		0.031							0.022				0.020
Yb	0.124	0.049	0.188	0.059					0.078	0.094	0.059			0.083
Lu	0.018	0.006	0.034	0.008					0.009	0.016	0.007			0.008
Y	2.75	1.04	4.43	1.25					1.83	3.07	1.39			3.35
Pb	0.49	0.79	9.28	15.63					0.73	0.27	1.86			0.52
U		0.008		0.017					0.005		0.004			
P		76.4		93.8					35.2		56.0			
As		0.06		0.36					0.13		0.08			
La/Sm	1.42	2.88	1.20	1.87					2.07	1.51	1.62			0.73
Sm/Yb	4.44	12.45	6.95	13.70					13.71	14.71	18.15			22.25
La/Yb	6.32	35.87	8.32	25.64					28.33	22.22	29.35			16.23
Eu/Eu*	0.87	7.04	1.35	2.26					1.35	1.08	1.35			0.72

Table T1 (continued).

Laboratory:	WHOI	CSIRO	WHOI	CSIRO	CSIRO	CSIRO	WHOI/SOC	CSIRO	CSIRO	SOC	SOC	WHOI	CSIRO
Hole:	1189A						1189B						
Core, section:	9R-1	10R-1	10R-1	13R-1	1R-1	1R-1	2R-1	3R-1	7R-1	7R-1	10R-1	10R-1	10R-1
Piece, interval (cm):	11, 72-77	3, 7-10	9, 73-77	1, 0-3	1A, 0-6	1B, 0-6	2,10-20	1, 0-11	1, 0-10	2, 12-22	1, 11-13	2, 14-24	3, 28-30
Depth (mbsf):	78.42	87.37	188.03	116.10	31.00	31.00	40.20	49.70	88.70	88.82	118.01	118.04	118.18
Description:	Breccia cement	Cavity lining, part of breccia cement	Breccia cement	Large crystal in vesicle	Anhy gangue: semimassive sulfide	Gyp gangue: semimassive sulfide	Anhy (gyp) breccia cement	90:10 gyp:anhy; breccia/stockwork vein	Breccia cement	Crustiform anhy with py	Open space anhy-py vein (≤4 mm thick)	Anhy-py vein	Coarse anhy vein
⁸⁷ Sr/ ⁸⁶ Sr	0.707483	0.706549	0.707566	0.705861	0.707580	0.707531	0.706225	0.706953	0.706993	0.706550	0.705558	0.706660	0.706442
δ ³⁴ S V-CDT (‰)				18.8	21.3	21.3	22.3	20.7	20.9				20.7
% seawater	65.7	43.5	67.6	25.4	67.9	66.8	35.2	53.5	54.4	43.6	16.8	46.3	40.8
Sr	2451		3287				1587			1673	991	1795	
D(Ca-Sr)	0.539		0.718				0.393			0.402	0.259	0.427	
Mg										671	243		
Li	0.084						0.076					0.0928	
Rb	0.069						0.130			0.087	0.090	0.095	
Cs	0.008						0.003			0.002	0.007	0.004	
Ba	2.08						32.83			14.07	23.42	11.80	
La	0.567						3.143			1.130	8.153	1.470	
Ce	1.117						7.873			3.033	18.360	3.316	
Pr	0.157						1.278			0.489	2.367	0.497	
Nd	0.713						5.892			2.638	10.703	2.200	
Sm	0.165						1.505			0.771	2.226	0.481	
Eu	0.068						0.535			0.218	1.101	0.214	
Gd	0.188						1.551			0.604	1.948	0.432	
Tb	0.025						0.184			0.081	0.228	0.049	
Dy	0.144						0.886			0.301	0.895	0.231	
Ho	0.027						0.142			0.035	0.170	0.036	
Er	0.065						0.301			0.068	0.366	0.076	
Tm										0.005	0.034		
Yb	0.036						0.149			0.024	0.182	0.040	
Lu	0.005						0.018			0.002	0.013	0.005	
Y	0.86						3.49			1.52	5.44	0.97	
Pb	0.23						0.57			5.24	1.51	1.32	
U	0.003						0.003					0.005	
P	28.8						28.2					50.6	
As	0.24						0.77					0.04	
La/Sm	2.22						1.35			0.95	2.36	1.97	
Sm/Yb	5.15						11.22			34.99	13.61	13.26	
La/Yb	11.40						15.12			33.12	32.18	26.15	
Eu/Eu*	1.17						1.06			0.94	1.58	1.40	

Table T1 (continued).

Laboratory:	WHOI/SOC	WHOI/SOC	SOC	SOC	CSIRO	WHOI	SOC	CSIRO	WHOI	SOC	WHOI/SOC	Sr duplicate	WHOI/CSIRO	SOC	
Hole:	1189B														
Core, section:	10R-1	10R-1	10R-1	11R-2	12R-1	12R-2	12R-3	14R-1	14R-1	14R-1	14R-1	14R-1	14R-2	14R-2	
Piece, interval (cm):	5, 38-50	5, 42-44	5, 42-44	8, 103-107	6, 96-98	1B, 9-12	2, 7-10	1, 0-10	12, 77-82	15, 112-115	17, 123-129	17, 123-129	1, 0-3	6, 23-28	
Depth (mbsf):	118.28	118.32	118.32	129.31	138.26	138.80	140.15	156.50	157.27	157.62	157.73	157.73	157.79	158.02	
Description:	Anhy vein	Anhy vein	Anhy-py vein (2 mm)	Anhy vein (1.5 mm)	Coarse anhy vein	Anhy vein	Anhy selvage on vesicular volc	Jog in anhy-qtz vein	Breccia cement	Crustiform anhy	Anhy cement	Anhy cement	Coarse anhy vein	Anhy vein	
⁸⁷ Sr/ ⁸⁶ Sr	0.706337	0.705799	0.707210	0.706866	0.707517	0.707860	0.706373	0.706331	0.706554	0.705451	0.706471	0.706522	0.706250	0.707029	
$\delta^{34}\text{S V-CDT}$ (‰)	22.1	21.4	21.4	22.4	21.1		21.1	21.3		22.2	20.7		20.4	22.1	
% seawater	38.1	23.6	59.5	51.4	66.5	74.0	39.1	38.0	43.7	13.7	41.6	42.9	35.9	55.3	
Sr	2440	1941	2030	1424			1625		1070	1475	1842			1904	
D(Ca-Sr)	0.598	0.499	0.459	0.332			0.397		0.257	0.390	0.446			0.438	
Mg		352		739			2327			139				1492	
Li			0.1						5.54		0.046		0.315		
Rb		0.055	0.123	0.087			0.021		0.400	0.066	0.091		0.075	0.123	
Cs			0.003	0.003					0.009	0.003	0.004		0.004	0.005	
Ba		64.27	20.09	41.31			30.02		4.24	14.71	62.59		10.90	7.21	
La		1.217	2.022	0.877			3.097		0.773	0.811	1.501		1.668	0.794	
Ce		2.882	4.943	2.532			7.117		1.627	1.688	2.587		5.217	1.697	
Pr		0.427	0.753	0.417			1.020		0.264	0.248	0.332		0.938	0.260	
Nd		2.278	3.327	2.400			5.435		1.291	1.321	1.292		4.565	1.338	
Sm		0.598	0.733	0.681			1.267		0.307	0.315	0.263		0.980	0.271	
Eu		0.220	0.264	0.136			0.657		0.072	0.039	0.733		0.627	0.087	
Gd		0.479	0.607	0.549			0.946		0.386	0.328	0.259		0.802	0.277	
Tb		0.045	0.067	0.081			0.113		0.051	0.051	0.027		0.088	0.041	
Dy		0.211	0.302	0.366			0.518		0.276	0.280	0.120		0.415	0.255	
Ho		0.028	0.044	0.054			0.082		0.051	0.057	0.017		0.064	0.037	
Er		0.070	0.088	0.099			0.145		0.124	0.116	0.036		0.131	0.168	
Tm		0.008		0.006			0.025			0.014				0.008	
Yb		0.041	0.044	0.062			0.089		0.066	0.070	0.021		0.064	0.088	
Lu		0.002	0.005	0.009			0.007		0.009	0.007	0.003		0.008	0.014	
Y		1.04	1.04	2.00			2.85		1.18	1.97	0.45		1.87	1.83	
Pb		1.62	0.98	2.86			0.65		4.01	2.10	1.97		0.35	3.34	
U			0.009						0.026		0.005		0.003		
P			39.2						40.8		162.2		59.5		
As			0.04						0.06		0.05		0.08		
La/Sm		1.31	1.78	0.83			1.58		1.63	1.67	3.69		1.10	1.89	
Sm/Yb		16.36	18.43	12.16			15.90		5.15	5.00	13.73		16.92	3.40	
La/Yb		21.50	32.82	10.12			25.09		8.37	8.33	50.60		18.58	6.44	
Eu/Eu*		1.21	1.18	0.66			1.76		0.64	0.37	8.48		2.10	0.97	